

Quantum Ghost Image Identification with Correlated Photon Pairs

Mehul Malik, Heedeuk Shin,* Malcolm O'Sullivan, Petros Zerom, and Robert W. Boyd

The Institute of Optics, University of Rochester, Rochester, New York 14627, USA

(Received 20 August 2009; published 23 April 2010)

Ghost imaging can be performed using either quantum or classical states of light that possess strong spatial correlations. In both cases, the image is formed by averaging over many optical events. Here we show that it is possible to distinguish an object from a preestablished basis set of objects by using a small number of position-correlated photon pairs produced by spontaneous parametric down-conversion. The signal photon is incident on one member of a set of spatially nonoverlapping objects. The “ghost” image information is impressed upon the spatially separated idler photon and is extracted by means of holographic filtering and coincidence detection. We were able to distinguish among sets of two and four spatially nonoverlapping objects with confidence levels higher than 87% and 81%, respectively. This method of ghost imaging can be performed in situations requiring extremely low light levels.

DOI: [10.1103/PhysRevLett.104.163602](https://doi.org/10.1103/PhysRevLett.104.163602)

PACS numbers: 42.50.Dv, 03.65.Ud, 42.30.-d, 42.65.Lm

In recent years, the phenomenon of entanglement has captured the imaginations of physicists and philosophers alike, and has made itself manifest as one of the most counterintuitive aspects of quantum mechanics. The strong correlations found in entangled photons have allowed great headway in experimental quantum mechanics, facilitating experiments ranging from the most fundamental to the very applied. Polarization-entangled photons have been used to obtain some of the most exacting experimental violations of Bell's inequality [1,2]. Time-energy entangled photons have found large application in various nonclassical techniques such as quantum cryptography [3] and quantum teleportation [4,5]. The strong spatial correlations found in position-momentum entangled photons have given rise to the field of quantum imaging and have allowed the development of techniques such as quantum lithography [6,7] and ghost imaging [8].

Ghost imaging, also known as coincidence imaging, was first implemented with position-momentum entangled photons [9]. An object is imaged by placing it in the path of one photon of an entangled pair. This signal photon, as it has come to be called, is then allowed to fall onto a spatially nonresolving bucket detector. As its name implies, the bucket detector collects all the signal photons that make it past the object. The idler photons, on the other hand, are incident upon a spatially resolving detector. A sharp image is obtained in the coincidence counts of the two detectors. The term “ghost image” was coined for this phenomenon based on the fact that the image was formed without directly obtaining any spatially resolved image information from the object itself [8].

It was soon shown that ghost imaging relied solely on the spatial correlations of the two light fields. The same effect was reproduced by using randomly but synchronously directed twin beams of classical light [10]. The only benefit of using entangled photons was found to be

that imaging could be performed both in the near and far fields, without having to change the source [11]. This is a direct consequence of the fact that entangled photons have strong correlations in both position and momentum, which correspond to correlations in the near and far fields, respectively. In the case of ghost imaging with an entangled source, the choice of whether to measure in the image plane or the diffraction pattern is left to the observer, instead of being determined by the source. Subsequently, even this property of ghost imaging with an entangled source was mimicked by using a pseudothermal source [12]. The twin speckle patterns created by shining an intense beam of light through a ground glass plate and a beam splitter were found to have strong spatial correlations in both the near and far fields [11].

In practice, both the quantum and thermal ghost imaging methods require the use of many single-photon pairs or random speckle patterns to obtain an image. Also, long processing times are needed for scanning an avalanche photodiode in the quantum case [9] or averaging many speckle patterns on a CCD camera in the thermal case [12]. These requirements have made the practical applicability of such schemes difficult. In some cases, however, it is useful to discriminate an object from a preestablished set of objects instead of imaging the object pixel by pixel. Recently, it has been shown that it is possible to impress and retrieve spatial information from a single photon using holographic filtering [13]. For a preestablished set of two spatially nonoverlapping objects, image information was impressed upon a single photon, which was then diffracted into a particular direction by a multiplexed hologram that acted as a “single-photon image sorter.” This is akin to matched-filtering techniques used in classical image processing [14].

In this Letter, we propose a quantum ghost imaging scheme that uses the aforementioned holographic filtering

technique to identify an object from a large basis set of objects. As a proof-of-principle experiment, we demonstrate this method for both a set of two and a set of four spatially nonoverlapping objects. We do so by replacing the CCD in the idler arm of the original ghost imaging setup [9] with a holographic sorter. The ghost image is obtained from the coincidence counts of the bucket detector and the beams diffracted by the hologram. In this manner, we are able to determine which object from our preestablished set is in the signal arm without directly acquiring any spatial information about it. In our analysis, we change the naming system by referring to the signal arm as the object arm and the idler arm as the ghost arm. The object arm is the path taken by the object photon and contains the object followed by the bucket detector. The ghost arm is the path taken by the ghost photon and contains a holographic sorter and single-photon detectors (Fig. 1).

Let us first describe the two-object case. The measurement in the object arm is carried out by the object-bucket detector combination. The object photon is either transmitted into the bucket detector, labeled *R* in Fig. 1, or is blocked by the object. The measurement in the ghost arm is carried out by the hologram-detectors combination. The ghost photon is diffracted into either detector *A* or *B*. If object *a* is present in the object arm and transmits an object photon into bucket detector *R*, the corresponding ghost photon will always be diffracted by the hologram into detector *A*. This is due to the strong position correlations between the two photons. A similar explanation holds for object *b*.

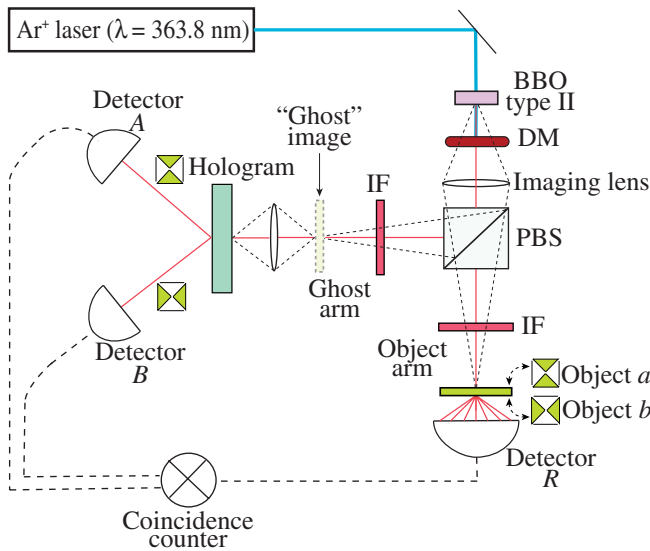


FIG. 1 (color online). Experimental setup. DM is a dichroic mirror for blocking the pump laser; IF is an interference filter with 10 nm bandwidth, centered at 727.6 nm. The dotted lines indicate the imaging process for a point object.

We now describe this effect more quantitatively. For simplicity, we assume a one-dimensional geometry. In the position basis, the two-photon state is written as

$$|\Psi\rangle = \iint dx_o dx_g f(x_o, x_g) |x_o\rangle |x_g\rangle. \quad (1)$$

Here $|x_o\rangle$ and $|x_g\rangle$ represent the positions of the object and ghost photon, respectively. $f(x_o, x_g)$ is a weighting function defined as

$$f(x_o, x_g) = \frac{2^{1/4}}{\sqrt{\pi w \sigma}} e^{-(x_o + x_g)^2 / 4w^2} e^{-(x_o - x_g)^2 / 2\sigma^2} \quad (2)$$

where w is the beam radius and σ is the transverse coherence length of the two-photon state [15]. Both parameters depend on the experimental geometry; we choose conditions such that w is very large and σ very small compared to the size of the objects.

We define \hat{o}_i and \hat{g}_j as projection operators in the object and ghost arms that collapse the object and ghost photons into states i and j , respectively. These are defined as

$$\hat{o}_i = \int dx_o t_i(x_o) |x_o\rangle \langle x_o|, \quad i = a \text{ or } b \quad (3)$$

$$\hat{g}_j = \int dx_g t_j(x_g) |x_g\rangle \langle x_g|, \quad j = a \text{ or } b \quad (4)$$

where $t_i(x_o)$ and $t_j(x_g)$ are binary transmission functions for the amplitude objects a or b , as shown in Fig. 1. The variables x_o and x_g are the transverse positions in the object plane and the ghost image plane, respectively.

The joint detection probability in the object and ghost arms can be expressed mathematically as

$$\langle \Psi | \hat{o}_i \hat{g}_j | \Psi \rangle = \sqrt{\frac{2}{\pi w^2}} \int dx_o t_i(x_o), \quad \text{if } i = j \quad (5)$$

and 0 otherwise. Equation (5) gives the probability of a coincidence count being registered between detector *R* and detector *A* or *B*. For the case $i = j$, this probability is proportional to the average transmission of the object being queried, and object identification is possible. For example, a coincidence count *R-A* indicates that object *a* is present in the object arm. For the case $i \neq j$, no coincidence count is registered. These detection scenarios are tabulated in Table I. The same theory can be extended to the case of four objects by expanding the object set to

$$i, j = a, b, c, \text{ or } d. \quad (6)$$

The above theory assumes the holographic sorter performs the operation \hat{g}_j reliably, which involves diffracting the ghost photon into the right detector with certainty. In principle, a holographic sorter can unambiguously distinguish among spatially nonoverlapping objects with high efficiency. For the general case of a set of overlapping objects, the efficiency with which a holographic sorter

TABLE I. Possible outcomes for two objects and a single-photon pair. R , A , and B are counts for the detectors shown in Fig. 1. R - A and R - B are coincidence counts between these detectors.

Object\detector	R	A	B	R - A	R - B
a	1	1	0	1	0
	0	0	1	0	0
b	1	0	1	0	1
	0	1	0	0	0

can distinguish objects is reduced. In such a situation, more than one photon is needed in order to unambiguously distinguish among objects. In our experiment, we construct holographic sorters for sets of two and four spatially non-overlapping objects as a proof of principle of our ghost image-identification scheme.

Our experimental setup for the two-object case is sketched in Fig. 1. The holographic sorter is created by multiplexing the two spatially nonoverlapping objects a and b with reference beams incident at different angles. It is recorded with a collimated HeNe laser at 633 nm on a silver-halide plate. The entangled photon pairs are created by degenerate spontaneous parametric down-conversion in a collinear type-II phase matched BBO crystal pumped by a cw beam from an argon-ion laser operating at a wavelength of 364 nm. The pump beam is well collimated with a divergence of less than 0.31 mrad and a beam waist of 3 mm. A dichroic mirror placed after the crystal blocks the pump laser light. A polarizing beam splitter separates the object photon from the ghost photon. The distance between the crystal and the object (and the ghost image plane) is 45 cm. The imaging condition is met by placing a 10-cm-focal-length lens 15 cm after the crystal. The ghost image plane then acts as a “virtual object” for the hologram. This imaging process is illustrated in Fig. 1 with dotted lines for a point object at the crystal. In the unfolded or Klyshko interpretation of the setup [8], one can understand the object as being imaged onto the crystal face, which is then imaged onto the ghost image plane, and consequently imaged onto the hologram. A more detailed theoretical analysis of the imaging process for entangled two-photon fields can be found in [16]. Perkin-Elmer avalanche photodiodes and a coincidence circuit with a window of approximately 12 ns are used for the detection.

In our experiment, overall detection efficiencies at detectors R , A , and B are about 13.8%, 1.2%, and 3.2%,

respectively, because of optical loss between the crystal and the detectors, detector efficiency, and diffraction efficiency of the hologram. Because of the limited detection efficiency, we have to wait until a coincidence count occurs. Measurements are performed using a 10 s integration, and the data are listed in Table II. When a coincidence count correctly identifies the object, we refer to it as a true case (A - a or B - b), and the opposite as a false case (A - b or B - a). The normalized experimental results for each object are graphed in Fig. 2(a). The data for each detector are normalized by the number of coincidence counts recorded by that detector for a true case. It is clear from this figure that our experimental system has high contrast between true and false cases. The percentage of true coincidences to the total number of coincidences (true + false) for a particular object is referred to as the confidence factor for that object. It is measured to be 87% for object a and 92% for object b . The ratio between total and accidental coincidence counts (T/A ratio) for each object-detector combination serves as a measure of the system fidelity [13] and is graphed in Fig. 2(b). The T/A ratio for the false cases is approximately unity, which indicates that almost all the counts in the false cases are due to accidental coincidences. This conclusion was checked by increasing the time window of the coincidence circuit. This points to the fact that we can obtain better discrimination results by using a narrower time window in the coincidence circuit. If a 500 ps coincidence window circuit were used, the accidental coincidence counts would be decreased by a factor of 25.6 for detectors R - A , and the confidence factor would then increase to 99.4%.

We now present our experimental results for the case of an object space of four objects. An angularly multiplexed hologram was created for the four spatially nonoverlapping objects shown in Fig. 3(c) using the same method as before. The normalized coincidence counts and the T/A ratios for each object-coincidence combination are plotted in Fig. 3. The data are normalized by the true-case-coincidence counts for each detector, which are 574, 379, 111, and 134 for detectors A , B , C , and D , respectively. The contrast between the true and false cases is very high and the T/A ratios indicate that the false cases are primarily due to accidental coincidence counts. We are able to discriminate between objects a , b , c , and d with confidence factors of 94.3%, 90%, 80.8%, and 84.7%, respectively.

Ghost image identification using a holographic sorter clearly has many advantages over other ghost imaging

TABLE II. Experimental data for the two-object case. All numbers are in counts/sec. R gives the bucket detector counts, A and B are the counts from the detectors in the hologram arm. R - A (tot.) and R - A (acc.) are total and accidental coincidence counts between detectors R and A . R - B (tot.) and R - B (acc.) are defined analogously for detectors R and B .

Object\detector	R	A	B	R - A (tot.)	R - B (tot.)	R - A (acc.)	R - B (acc.)	Confidence
a	234 979	87 614	237 933	2683 ± 56	611 ± 31	264 ± 2	576 ± 4	87%
b	351 510	85 641	240 335	386 ± 20	7458 ± 67	386 ± 2	870 ± 3	92%

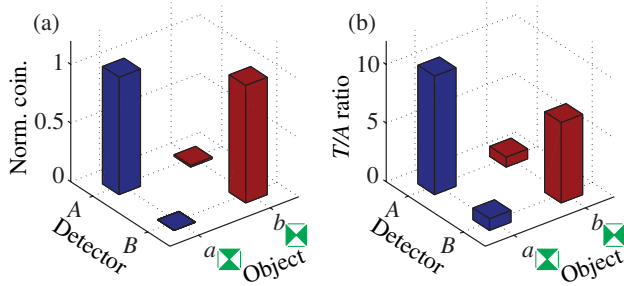


FIG. 2 (color online). Image-identification results for the two-object case. (a) Data for each object-detector combination are normalized by the maximum coincidence count for the corresponding object. (b) T/A ratio is calculated by dividing the total coincidences by the accidental coincidences for each object-detector combination.

schemes. First, a hologram provides an all-optical method of sorting images that can overcome the limitations of slow CCD frame rates [17]. Second, distinguishing among objects of a known set is much faster than building an image pixel by pixel. This approach has practical applications in situations where the objects to be distinguished fall into a relatively small class of objects. Third, an advantage of using quantum ghost image identification appears in the applicability of this method when extremely low light levels are required. One can classify this as a type of “stealth imaging,” where a minimum number of photons is used in order to avoid optical eavesdropping or letting the object become aware of its detection. The small number of photons used in quantum ghost image-identification make it an excellent candidate for such imaging schemes.

Matched filters have been used for pattern recognition for many years [14]. Highly overlapping objects can be sorted with a high confidence factor using matched filters made with holograms [18]. While our experiment ad-

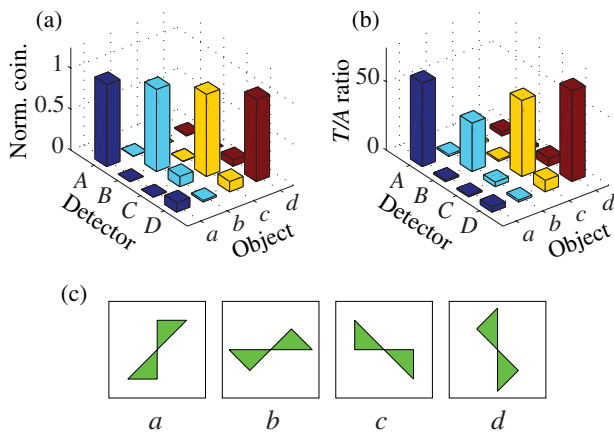


FIG. 3 (color online). (a) and (b) Graphs of image-identification results for the four-object case. (c) The four spatially nonoverlapping objects used in our experiment.

resses only nonoverlapping amplitude objects, in principle it is possible to construct matched filters that distinguish among complicated and overlapping objects. However, as mentioned earlier, the efficiency of the identification process is reduced for such sets of objects, and more than one photon pair is needed to distinguish unambiguously among them [19].

In conclusion, we have shown that it is possible to discriminate among nonoverlapping objects using a small number of correlated photon pairs, without gaining any spatially resolved information about the objects themselves. Although we have performed this experiment for object spaces of two and four objects, it is possible to expand the size of the object space markedly. Multiplexed holograms have been designed to store as many as 10 000 images [20]. However, as the object space increases, limitations on coincidence counts will be imposed by large cross talk and low diffraction efficiency. The possibility of using thick holograms to remedy such problems is a topic that we are currently pursuing.

This work was supported by the U.S. Army Research Office under a MURI grant and by DARPA/DSO.

*hshin@optics.rochester.edu

- [1] J. S. Bell, *Physics* (Long Island City, N.Y.) **1**, 195 (1964).
- [2] J. Clauser, M. A. Horne, A. Shimony, and R. A. Holt, *Phys. Rev. Lett.* **23**, 880 (1969).
- [3] C. Bennett *et al.*, *J. Cryptol.* **5**, 3 (1992).
- [4] D. Bouwmeester *et al.*, *Nature* (London) **390**, 575 (1997).
- [5] A. Furusawa *et al.*, *Science* **282**, 706 (1998).
- [6] A. N. Boto *et al.*, *Phys. Rev. Lett.* **85**, 2733 (2000).
- [7] M. D’Angelo, M. V. Chekhova, and Y. Shih, *Phys. Rev. Lett.* **87**, 013602 (2001).
- [8] D. V. Strekalov, A. V. Sergienko, D. N. Klyshko, and Y. H. Shih, *Phys. Rev. Lett.* **74**, 3600 (1995).
- [9] T. B. Pittman, Y. H. Shih, D. V. Strekalov, and A. V. Sergienko, *Phys. Rev. A* **52**, R3429 (1995).
- [10] R. S. Bennink, S. J. Bentley, and R. W. Boyd, *Phys. Rev. Lett.* **89**, 113601 (2002).
- [11] A. Gatti, E. Brambilla, M. Bache, and L. A. Lugiato, *Phys. Rev. Lett.* **93**, 093602 (2004).
- [12] F. Ferri *et al.*, *Phys. Rev. Lett.* **94**, 183602 (2005).
- [13] C. J. Broadbent, P. Zerom, H. Shin, J. C. Howell, and R. W. Boyd, *Phys. Rev. A* **79**, 033802 (2009).
- [14] G. L. Turin, *IRE Trans. Inf. Theory* **6**, 311 (1960).
- [15] K. W. Chan, J. P. Torres, and J. H. Eberly, *Phys. Rev. A* **75**, 050101(R) (2007).
- [16] A. Abouraddy, B. Saleh, and A. Sergienko, *J. Opt. Soc. Am. B* **19**, 1174 (2002).
- [17] G. He, X. Wang, D. Li, and J. Hu, *Optik* **119**, 548 (2008).
- [18] J. W. Goodman, *Introduction to Fourier Optics* (Roberts and Company, Greenwood Village, CO, 2005), 3rd ed., Chap. 8.
- [19] G. M. Morris, *Appl. Opt.* **23**, 3152 (1984).
- [20] X. An, D. Psaltis, and G. W. Burr, *Appl. Opt.* **38**, 386 (1999).